Published in final edited form as:

J Physiol. 2020 March ; 598(5): 987–998. doi:10.1113/JP278788.

HD-tDCS Dissociates Fronto-Visual Theta Lateralization during Visual Selective Attention

Rachel K. Spooner[1,2], **Jacob A. Eastman**[1,2], **Michael T. Rezich**[1,2], **Tony W. Wilson**[1,2]

[1]Department of Neurological Sciences, University of Nebraska Medical Center (UNMC), Omaha, NE USA 68198

[2]Center for Magnetoencephalography, UNMC, Omaha, NE USA 68198

Abstract

Studies of visual attention have implicated oscillatory activity in the recognition, protection, and temporal organization of attended representations in visual cortices. These studies have also shown that higher-order regions such as the prefrontal cortex are critical to attentional processing, but far less is understood regarding prefrontal laterality differences in attention processing. To examine this, we selectively applied high-definition transcranial direct-current stimulation (HD-tDCS) to the left or right dorsolateral prefrontal cortex (DLPFC). We predicted that HD-tDCS of the left versus right prefrontal cortex would differentially modulate performance on a visual selective attention task, and alter the underlying oscillatory network dynamics. Our randomized crossover design included 27 healthy adults that underwent three separate sessions of HD-tDCS (sham, left- and right-DLPFC) for 20 minutes. Following stimulation, participants completed an attention paradigm during magnetoencephalography (MEG). The resulting oscillatory dynamics were imaged using beamforming, and peak task-related neural activity was subjected to dynamic functional connectivity analyses to evaluate the impact of stimulation site (i.e., left and right DLPFC) on neural interactions. Our results indicated that HD-tDCS over the left DLPFC differentially modulated right fronto-visual functional connectivity within the theta band compared to HD-tDCS of the right DLPFC and further, specifically modulated the oscillatory response for detecting targets among an array of distractors. Importantly, these findings provide network-specific insight into the complex oscillatory mechanisms serving visual selective attention.

Corresponding Author: Tony W. Wilson, Center for Magnetoencephalography, University of Nebraska Medical Center, 988422 Nebraska Medical Center, Omaha, Nebraska 68198-8422, twwilson@unmc.edu, Phone: (402) 552-6431.

Author Contributions

Rachel K. Spooner: Study concept and design, analysis and interpretation of data, drafting of the manuscript, and statistical analysis.
Jacob A. Eastman: Acquisition of data, drafting of the manuscript.
Michael T. Rezich: Acquisition of data, drafting of the manuscript.
Tony W. Wilson: Study concept and design, analysis and interpretation of data, acquisition of data, drafting of the manuscript, statistical analysis and study supervision.
All authors approved the final version of the manuscript and agree to be accountable for all aspects of the work. All data was collected at the MEG Center at the University of Nebraska Medical Center, Omaha, NE, USA. All persons designated as authors qualify for authorship, and all those who qualify for authorship are listed.

Competing Interests Statement

The authors disclose no financial, commercial or institutional conflicts of interest.

Keywords

magnetoencephalography; Flanker task; theta oscillations; functional connectivity

Introduction

The ability to allocate attention to pertinent information within a larger visual field, while simultaneously inhibiting distracting or irrelevant information is essential to carrying out goal-directed behaviors. Such selective processing of visual information to adapt to current goals has been attributed to a network of regions encompassing prefrontal, parietal, and visual cortices. Specifically, prefrontal cortices have been implicated in the top-down modulation of posterior, sensory responses in order to achieve rapid adjustments in behavior. In the context of visual interference, medial, ventral and lateral prefrontal cortices may be preferentially active to support different aspects governing response interference. For example, there is a wealth of literature implicating medial prefrontal cortex and anterior cingulate in the active monitoring of conflict or error produced by interfering stimuli (Botvinick *et al.*, 1999; Hazeltine *et al.*, 2000; van Veen *et al.*, 2001; Bunge *et al.*, 2002; Lau *et al.*, 2006). In contrast, the lateral PFC may play an important role in the suppression of distracting information, while the ventral PFC acts as a reorienting system to salient stimuli (Corbetta & Shulman, 2002; Corbetta *et al.*, 2008; Paneri & Gregoriou, 2017). Further, these regions appear to be intricately connected to posterior cortex including parietal regions and bottom up processors, with hierarchical organization of these networks implicating PFC specifically in top-down control mechanisms (Miller, 2000; Brass *et al.*, 2005; Miller & D'Esposito, 2005). Importantly, while neuropsychological, lesion and neuroimaging studies have largely characterized the spatial extent of PFC involvement during cognitive processes such as visual selective attention (Botvinick *et al.*, 1999; Hazeltine *et al.*, 2000; Bunge *et al.*, 2002; Lau *et al.*, 2006; McDermott *et al.*, 2017; Embury *et al.*, 2018; Lew *et al.*, 2018; McDermott *et al.*, 2019), the underlying oscillatory dynamics and dynamic connectivity serving such processes are less well understood. Such data would be integral to revealing the mechanistic recruitment of neural networks that govern behavioral adaptation during interference.

Previous work has repeatedly shown prefrontal and visual theta oscillatory activity during visual attention tasks. Specifically, a role of prefrontal theta oscillations has been identified during attention, executive function, and working memory tasks (Jensen & Tesche, 2002; Cavanagh *et al.*, 2009; Cohen & Cavanagh, 2011; Nigbur *et al.*, 2011; Nigbur *et al.*, 2012; Cavanagh & Frank, 2014). Additionally, lateral and medial PFC theta oscillations have been linked to cognitive control, specifically during active monitoring of response conflict, such that increases in prefrontal theta activity are notable during times of increasing interference (Cavanagh *et al.*, 2009; Cohen & Cavanagh, 2011; Nigbur *et al.*, 2011; Nigbur *et al.*, 2012; Cavanagh & Frank, 2014; Cohen & van Gaal, 2014; Padrão *et al.*, 2015). In contrast, theta activity in visual cortices may aid in the temporal organization and segmentation of visual input (Jensen & Tesche, 2002; Busch *et al.*, 2009; Verbruggen *et al.*, 2010; Landau & Fries, 2012; Landau *et al.*, 2015). When considering the dynamic interplay between these cortical regions, recent evidence suggests that theta oscillations in prefrontal and visual cortices are

dynamically connected and further, greater synchronicity is related to faster visuospatial discrimination (Wiesman *et al.*, 2017; Wiesman *et al.*, 2018). Together, these data provide strong support for dynamic interactions in the theta range, however, it is uncertain how homologous fronto-visual oscillations might interact during times of visual selective attention.

Neuromodulatory methods such as transcranial direct current stimulation (tDCS) provide a unique venue to elucidate the neural mechanisms serving cognitive processes and behavioral performance. While the current supplied by tDCS is too minute to elicit neuronal firing, increasing evidence supports its capacity to alter the local ionic environment (Nitsche & Paulus, 2000, 2001; Nitsche *et al.*, 2003; Bikson *et al.*, 2004; Radman *et al.*, 2007; Reato *et al.*, 2010; Coffman *et al.*, 2014; Filmer *et al.*, 2014; Bachtiar *et al.*, 2015; Fertonani & Miniussi, 2017; Kronberg *et al.*, 2017). Conventional applications of tDCS utilize two large (~35 cm^2) electrodes to administer low amplitude currents in a bipolar fashion, which creates a semi current-loop running from anode to cathode through intervening brain tissues. While conventional administration of tDCS remains the most common, the spatial extent of the electrical changes is quite large, making its effects on cognitive performance difficult to predict and this often complicates interpretation (Edwards *et al.*, 2013; Kuo *et al.*, 2013). Fortunately, the use of high definition tDCS (HD-tDCS) partially circumvents this issue through a 4×1 electrode montage, with a central electrode surrounded by four electrodes of opposing polarity. Such design provides a more focal and potentially more selective form of neuromodulation (Edwards *et al.*, 2013; Kuo *et al.*, 2013; Turski *et al.*, 2017). For example, HD-tDCS of the motor cortex has been shown to increase cortical excitability for prolonged periods directly beneath the site of stimulation, as measured by motor evoked potentials (MEPs) using transcranial magnetic stimulation (TMS; (Kuo *et al.*, 2013). In regard to the degree of focality, studies have shown that HD-tDCS directly over the motor cortex at intensities derived from current density modeling elicits MEPs, while such predicted stimulation intensities at sites just anterior and posterior of the motor cortex do not elicit MEPs (Edwards *et al.*, 2013). Importantly, tDCS has been found to modulate behavioral performance across a variety of cognitive domains, depending on the location of stimulation, and further it differentially influences the neural oscillations essential to these processes (Hanley *et al.*, 2016; Marshall *et al.*, 2016; Heinrichs-Graham *et al.*, 2017; Wiesman *et al.*, 2018; Wilson *et al.*, 2018; McDermott *et al.*, 2019).

In this study, we use HD-tDCS and magnetoencephalography (MEG) to investigate dynamic functional connectivity in the theta range among prefrontal and visual nodes during attentional processing. Specifically, 20 minutes of anodal HD-tDCS was administered over the left and right dorso-lateral prefrontal cortex (DLPFC) followed by subsequent MEG recording of neurophysiological activity during a letter-based Eriksen Flanker task. Consistent with previous findings, we hypothesized differential modulation of fronto-visual dynamic connectivity based on stimulation montage (i.e., left-, right-anodal DLPFC, and sham), specifically between sites of neuromodulation and task-induced activity in visual cortex. Importantly, we predicted that the dynamic changes in fronto-visual connectivity would significantly affect behavior and more specifically, the impact of interfering stimuli.

Methods

Ethical Approval

This experimental work conformed to the standards set by the Declaration of Helsinki, except for registration in a database. The University of Nebraska Medical Center's Institutional Review Board approved the study protocol. A full description of the study was given to all participants, followed by written informed consent which was obtained following the guidelines of the University of Nebraska Medical Center's Institutional Review Board.

Participants

Twenty-seven healthy young adults (M = 23.6, 11 females) participated in this study. Exclusion criteria included any medical illness affecting CNS function (e.g., psychiatric and/or neurological disease), history of head trauma, current substance abuse, and metal ferromagnetic implants that could disrupt the MEG recordings.

Transcranial Direct Current Stimulation (tDCS)

A repeated measures crossover design was chosen for this study, where participants completed three separate stimulation configurations at least one week apart from one another (M = 10.8 days, SD = 7.2 days; Figure 1). High-definition (HD) anodal tDCS was administered to the left and right dorsolateral prefrontal cortex (DLPFC). Stimulation configurations (i.e., left-, right-anodal DLPFC, and sham) were pseudo-randomized across visits and participants were blinded to each montage, as were all researchers associated with data analyses. With exception of stimulation montage (i.e., left or right DLPFC) and condition (i.e., active or sham), all participants completed the same experimental protocol.

Across all three visits, a 4×1 HD tDCS system was positioned over the left or right DLPFC with the central electrode assigned anodal polarity and the surrounding reference electrodes assigned cathodal polarity. Each electrode was secured atop electroconductive Signa gel using an EEG cap and positioned using the International 10/20 system (i.e., F3 and F4 for left and right DLPFC, respectively; (Jasper, 1958), which is commonly employed in EEG, fNIRS, and tDCS studies (e.g., (Wilson *et al.,* 2014)). Importantly, a probabilistic distribution of cortical projection points has been developed by Okamoto et al. to transform scalp-based International 10/20 system coordinates into Montreal Neurological Institute (MNI) based coordinates with relatively high accuracy (average standard deviation ~ 8 mm) (Okamoto *et al.*, 2004; Okamoto & Dan, 2005). Thus, we computed the coordinates of each electrode in the International 10/20 system, and then used the transformation methods provided by Okamoto et al. to obtain the MNI coordinates that corresponded to these scalp-based locations. This indicated that the central anode in our 4×1 array was over the left or right DLPFC. In the sham condition, the electrodes were in the same locations and pseudo-randomized across participants whether they were over the left or right DLPFC.

Participants in each anodal stimulation condition (i.e., the left and right DLPFC) underwent 20 minutes of 2.0 mA direct-current stimulation, plus a 30 s ramp-up period in addition to stimulation, while completing a battery of neuropsychological measures to stay engaged

during stimulation protocols. The current intensity used for this study (i.e., 2.0 mA) was chosen based on previous literature with the goal of maximizing the effect of stimulation. Briefly, these studies suggest that greater levels of cortical excitability (MEPs) were evident following tDCS applications using greater current intensities (e.g., 1.0 or 2.0 mA) (Nitsche & Paulus, 2000; Nitsche *et al.*, 2008; Chew *et al.*, 2015). Three-dimensional current density modeling of this stimulation was performed using a finite-element model (FEM) of current flow to verify that left and right DLPFC were being targeted effectively (Kempe *et al.*, 2014; Ruffini *et al.*, 2014). Briefly, current density modeling was computed using Soterix HD Explore software and was based on the following conductivity parameters derived from the literature: GM = .276, WM = .126, CSF = 1.65, skull = 0.01, skin = 0.465, air = 1×10^{-7}, gel = 0.3, electrodes = 5.8×10^{7} (Datta *et al.*, 2009; Datta *et al.*, 2011; Datta *et al.*, 2012; Huang *et al.*, 2013; Huang *et al.*, 2018). The sham group received the same neuropsychological battery for 20 minutes, but no stimulation outside of the 30 s ramp up period. A Soterix Medical (New York, New York, USA) tDCS system and 4×1 HD adapter was used for stimulation. Following HD-tDCS, participants underwent MEG recording that lasted approximately 14 minutes. The total setup took about 10 minutes from the stop of stimulation to the initiation of the MEG session, which was by design given the findings of Kuo et al. indicating that the level of cortical excitability peaks about 20 minutes after cessation of tDCS, and slowly diminishes around 70–90 minutes following tDCS cessation (Kuo *et al.*, 2013).

Experimental Paradigm

Participants were seated in a nonmagnetic chair with their head positioned within the MEG helmet-shaped sensor array. Participants performed a letter-based version of the Eriksen flanker task (Eriksen & Eriksen, 1974). Each trial began with a fixation cross presented for 1450–1550 ms. A row of five letters (i.e., O and/or Q) was then presented for 2500 ms and participants were instructed to indicate with their right hand whether the middle letter was an O (index finger) or Q (middle finger). Participants completed 200 pseudo-randomized trials equally split between congruent and incongruent conditions (Figure 1), with O and Q letters being equally distributed across experimental conditions. The MEG recording lasted approximately 14 minutes.

MEG Data Acquisition and Coregistration with Structural MRI

All recordings were performed in a one-layer magnetically-shielded room with active shielding engaged for environmental noise compensation. With an acquisition bandwidth of 0.1–330 Hz, neuromagnetic responses were sampled continuously at 1 kHz using an Elekta MEG system (Elekta, Helsinki, Finland) with 306 magnetic sensors, including 204 planar gradiometers and 102 magnetometers. Throughout data acquisition, participants were monitored using a real-time audio-video feed from inside the magnetically-shielded room. MEG data from each participant were individually corrected for head motion and subjected to noise reduction using the signal space separation method with a temporal extension (Taulu *et al.*, 2005; Taulu & Simola, 2006). Each participant's MEG data were coregistered with structural T1-weighted MRI data prior to source space analyses using BESA MRI (Version 2.0). Structural MRI data were aligned parallel to the anterior and posterior commissures and transformed into standardized space. After beamformer analysis, each

subject's functional images were also transformed into standardized space using the transform applied to the structural MRI volume and spatially resampled.

MEG Preprocessing, Time-Frequency Transformation, and Sensor-Level Statistics

Cardiac artifacts were removed from the data using signal-space projection (SSP) and the projection operator was accounted for during source reconstruction (Uusitalo & Ilmoniemi, 1997). Epochs were of 2000 ms duration, with 0 ms defined as the onset of the stimulus and the baseline being the −450 to −50 ms window. Epochs containing artifacts were rejected based on a fixed threshold method, supplemented with visual inspection. On average, 174 total trials (87 congruent and 87 incongruent) per participant were used for further analysis and the average number of trials accepted did not statistically differ by stimulation configurations.

Artifact-free epochs were transformed into the time-frequency domain using complex demodulation, and the resulting spectral power estimations per sensor were averaged over trials to generate time-frequency plots of mean spectral density. The sensor-level data per time-frequency bin was normalized using the mean power per frequency during the −450 to −50 ms baseline time period. The specific time-frequency windows used for imaging theta oscillatory activity were determined by statistical analysis of the sensor-level spectrograms across all participants. Each data point in the spectrogram was initially evaluated using a mass univariate approach based on the GLM. To reduce the risk of false positive results while maintaining reasonable sensitivity, a two-stage procedure was followed to control for Type 1 error (Maris & Oostenveld, 2007). Briefly, paired-samples t-tests were conducted on each data point and the resulting spectrogram of t-values was thresholded at $p < .005$ to define time-frequency bins containing potentially significant oscillatory deviations across all participants. In stage two, time-frequency bins that survived this threshold were clustered with temporally and/or spectrally neighboring bins that were also significant, and a cluster value was derived by summing all of the t-values of all data points in the cluster. Nonparametric permutation testing was then used to derive a distribution of cluster-values and the significance level of the observed clusters (from stage one) were tested directly using this distribution (Ernst, 2004; Maris & Oostenveld, 2007). For each comparison, at least 10,000 permutations were computed to build a distribution of cluster values. Further details of this method and our processing pipeline can be found in recent papers (Wiesman *et al.*, 2017; Spooner *et al.*, 2018a; Spooner *et al.*, 2018b; Wiesman *et al.*, 2018; McDermott *et al.*, 2019; Spooner *et al.*, 2019).

MEG Beamformer Imaging and Statistics

Cortical networks were imaged through the dynamic imaging of coherent sources (DICS) beamformer (Van Veen *et al.*, 1997; Gross *et al.*, 2001), which employs spatial filters in the time-frequency domain to calculate source power for the entire brain volume. Such images are typically referred to as pseudo-t maps, with units (pseudo-t) that reflect noise-normalized power differences (i.e., active versus passive) per voxel. MEG pre-processing and imaging used the Brain Electrical Source Analysis (Version 6.1; BESA) software. Normalized source power was computed for the selected time-frequency periods (see Results) over the entire brain volume per participant at 4.0 × 4.0 × 4.0 mm resolution. The resulting beamformer

images were averaged across all participants, HD-tDCS configurations (i.e., left-, right-anodal DLPFC and sham) and task conditions (i.e., congruent and incongruent trials) to assess the neuroanatomical basis of the significant theta oscillatory responses to the stimulus presentation identified through the sensor-level analysis.

Functional Connectivity Analyses

In order to evaluate dynamic connectivity between neural regions associated with selective attention processing and the site of neurostimulation, we computed phase coherence within the respective theta frequency band derived from our statistically-defined clusters. Specifically, phase coherence was evaluated between prefrontal sites of electrical stimulation (i.e., left and right DLPFC) and functionally-defined peak activity in primary visual cortices associated with target processing. To compute phase coherence, we extracted the phase-locking value (PLV) using the method described by Lachaux et al (Lachaux *et al.*, 1999). The PLV reflects the inter-trial variability of the phase relationship between pairs of brain regions as a function of time. Values close to 1 indicate strong synchronicity (i.e., phase-locking) between the two brain regions within the specific time window across trials, whereas values close to 0 indicate substantial phase variation between the two signals, and thus, weak synchronicity (connectivity) between the two regions. To determine whether task-related functional connectivity differed significantly as a function of HD-tDCS configuration and selective attention (i.e., interference), values from the extracted PLV time series per pair of peaks were averaged across the task-active period (i.e., 0–500 ms). The computed values for active stimulation were normalized by dividing each active condition by sham, thus values greater than 1 are indicative of greater PLV in active conditions relative to sham. No effect of hemisphere for visual responses was hypothesized, however extensive literature substantiates the functional laterality of the prefrontal cortices. To account for this, task-active PLV values were extracted from the peak sources of activity in the visual cortex and collapsed across. However, bilateral activity was investigated for frontal sources as a factor in repeated measures ANOVA. Of note, potential confounding sources common in functional connectivity analyses (i.e., relative power at the source interrogated) were controlled for in all analyses (Brookes *et al.*, 2011).

These values were then compared using a 2×2×2 repeated measures ANOVA, with tDCS configuration (i.e., left- and right-anodal DLPFC), task condition (i.e., congruent and incongruent), and network (i.e., left or right DLPFC-bilateral visual cortices) as within-subjects factors. Finally, to evaluate the association between neural indices and performance on the task, Pearson correlations between PLV and behavioral metrics were conducted.

Results

Current Modeling and Selective Attention Performance

All 27 participants were able to successfully complete the neuromodulatory and MEG portions of the study. However, two participants were excluded from final analyses due to excessive artifacts in their MEG data and/or technical problems. The remaining 25 participants (10 females) had a mean age of 23.4 years and 24 were right-handed. As described in the methods section, participants underwent three separate HD-tDCS montages

(i.e., left- and right-anodal DLPFC, and sham; Figure 1), each applying a 4×1 HD electrode distribution over left or right DLPFC cortices. Three-dimensional current distribution modeling revealed a focal distribution, with field intensity strongest in the left and right DLPFC (Figure 1). After stimulation, participants completed a letter-based Eriksen Flanker task during MEG. Irrespective of HD-tDCS montage, participants performed well on the task, with a mean overall accuracy of 98.4%. Importantly, across all HD-tDCS montages, there was a significant effect of stimulus interference on reaction time ($t(74) = 4.82$, $p < .001$) and accuracy ($t(74) = 2.41$, $p = .018$). Specifically, participants were slower to respond ($M = 768.0$ ms, $SD = 141.3$ ms) and less accurate ($M = 98.2\%$, $SD = 3.4\%$) for incongruent trials relative to congruent trials (reaction time: $M = 750.7$ ms, $SD = 143.7$ ms; accuracy: $M = 98.6\%$, $SD = 2.9\%$; Figure 1). Finally, there was no significant effect of tDCS montage on reaction time ($F(73) = 1.37$, $p = .264$) or accuracy ($F(73) = .752$, $p = .477$).

Theta Oscillatory Dynamics during Selective Attention

Given the previous literature implicating theta oscillations in prefrontal and visual cortices during attentional processing, we limited our analyses to a statistically-derived window of oscillatory activity in the theta band. Robust synchronizations in the theta band (4–8 Hz) were found in many sensors near the occipital and parietal cortices across all task conditions and HD-tDCS montages ($p < .001$, corrected, Figure 2). Briefly, strong theta increases began shortly after stimulus onset and tapered off about 250 ms later (i.e., 0–250 ms; $p < .05$, corrected). To identify the brain regions generating the significant sensor-level oscillations, time frequency windows of interest were imaged using a beamformer. Strong increases in theta were observed during the first 250 ms after stimulus onset in bilateral primary visual cortices. Peak locations were virtually identical across task conditions and HD-tDCS montages. As described in the methods, these images were grand averaged across all participants, task conditions and HD-tDCS montages (Figure 2). We next computed phase coherence between sites of prefrontal stimulation (i.e., left and right DLPFC) and peak responses in bilateral primary visual cortices following stimulus onset in the theta band.

HD-tDCS Differentially Modulates Fronto-Visual Network Dynamics

Fronto-visual network dynamics were evaluated as a function of stimulation montage using phase coherence between prefrontal sites of HD-tDCS and peak task-related activity. Briefly, prefrontal nodes were identified based on coordinates derived from Okamoto and colleagues, who developed a probabilistic distribution of head surface and cortical projection points based on the International 10/20 system (Okamoto *et al.*, 2004; Okamoto & Dan, 2005). Phase coherence during task performance was then computed using these left and right DLPFC sites and the functionally-defined peak voxels in bilateral occipital cortices. Finally, the computed phase coherence values for active stimulation were normalized by dividing each active condition (i.e., left and right-DLPFC) by sham; thus, values greater than 1 are indicative of greater phase coherence in active conditions relative to sham. These data underwent 2×2×2 repeated measures ANOVA with tDCS montage (i.e., left and right-active), task condition (i.e., congruent and incongruent), and network (i.e., left DLPFC-bilateral visual cortices, right DLPFC-bilateral visual cortices). Interestingly, fronto-visual connectivity was significantly modulated by stimulation montage in a lateralized fashion, as there was a significant 3-way montage × condition × network interaction ($F(24) = 4.574$, p

= .043). Post hoc analyses of this interaction indicated that participants exhibited greater phase coherence in the right DLPFC-bilateral visual network during processing of incongruent trials following stimulation over the left DLPFC compared to stimulation over the right (p = .043). This increase in fronto-visual connectivity by HD-tDCS was specific to right-lateralized fronto-visual networks, as no differences were seen in left DLPFC-bilateral visual networks. Importantly, source power differences were controlled for in all functional connectivity analyses, and repeating the ANOVA using the non-normalized phase coherence data (i.e., including sham as a condition) yielded virtually identical results.

Finally, we evaluated the relationship among connectivity indices and behavioral performance using correlation analyses. Interestingly, dynamic increases in fronto-visual connectivity correlated strongly with decreased reaction time on the task after stimulation of the left DLPFC (left DLPFC-bilateral visual: r = −.43, p = .03, right DLPFC-bilateral visual: r = −.43, p = .03), but not the right DLPFC (p's > .25).

Discussion

By stimulating the prefrontal cortex and subsequently imaging the neural oscillations involved in visual selective attention, we have discovered that connectivity along specific prefrontal-visual pathways is selectively amplified during the processing of interfering stimuli. Specifically, stimulating over the left DLPFC dynamically increased right fronto-visual theta connectivity relative to stimulation over the right DLPFC, and connectivity along all pathways was significantly correlated with behavioral performance following left DLPFC. The implications of these novel findings are described below.

Visual selective attention is often described as the capacity to discriminate and focus on visual features of interest within the larger visual field, while simultaneously inhibiting distracting visual input (Driver, 2001; Carrasco, 2011). Previous work has implicated a variety of regions important for this process, including but not limited to: lateral prefrontal cortex, medial prefrontal, anterior cingulate, superior parietal lobules, and the supplementary motor area (Botvinick *et al.*, 1999; Hazeltine *et al.*, 2000; van Veen *et al.*, 2001; Bunge *et al.*, 2002; Lau *et al.*, 2006; McDermott *et al.*, 2017; Embury *et al.*, 2018; Lew *et al.*, 2018; Wilson *et al.*, 2018). Previous studies using modifications of the Eriksen Flanker task have primarily characterized the role of medial prefrontal and anterior cingulate in conflict and error monitoring, while the role of more lateralized nodes is less well understood. Reviews of the functional specialization of PFC, specifically in the context of visual attention, have suggested that increased neural activity in the lateral PFC corresponds to target representations along with decreases during distractor representations, and that lesions of this area result in increased distractibility during cognitive performance (Chao & Knight, 1995; Lennert & Martinez-Trujillo, 2011; Suzuki & Gottlieb, 2013; Gregoriou *et al.*, 2014; Paneri & Gregoriou, 2017). These descriptions of lateral PFC involvement align nicely with our tDCS-induced changes in the right lateral PFC's connectivity with posterior regions.

Importantly, our study design preferentially targeted left and right DLPFC as defined by the International 10/20 system (Jasper, 1958) and supported the necessity of lateral PFC involvement during visual selective attention. Specifically, we found that right DLPFC-

bilateral visual connections, but not left DLPFC-bilateral visual connections, were selectively modulated based on the laterality of DLPFC stimulation. Finally, the left DLPFC-bilateral visual networks that were interrogated in the current study were not impacted by stimulation and had seemingly no effect on neural response to distracting stimuli, suggesting a potential laterality of the prefrontal cortex even after controlling for source power. Previous investigations of laterality in prefrontal cortices have dissociated the left and right DLPFC during a variety of cognitive tasks (Kaller *et al.*, 2011). Notably, right-lateralized recruitment of neural networks has been repeatedly reported during attentional processing, specifically during times of target detection and attentional shifts (Heilman & Van Den Abell, 1980; Posner & Petersen, 1990; Corbetta *et al.*, 2000; Shulman *et al.*, 2010). The data presented in the current study expand well upon these previous findings by selectively modulating local activity and seeing how these brain regions respond to identical cognitive demands. Essentially, our data suggest that a right-lateralized fronto-bilateral visual network is crucial during visual selective attention as it was selectively disrupted by the stimulation, especially during the distracting incongruent trials, and such stimulation also disrupted the correlation between neural activity and behavioral performance on the task. Although it is worth noting that our sample size (i.e., 25 participants) may have been underpowered to detect all network-level neuro-behavioral correlations and future investigations in this area are necessary.

Of exceptional relevance to the current study is the role of theta oscillations in prefrontal and visual networks. In particular, theta activity in visual cortices is thought to reflect an introductory stage of the visual processing stream, specifically the temporal encoding and organization of visual information (Jensen & Tesche, 2002; Busch *et al.*, 2009; Verbruggen *et al.*, 2010; Landau & Fries, 2012; Landau *et al.*, 2015). For example, Wiesman et al. characterized the spatiotemporal and spectral integrity of networks serving visuospatial attention. Importantly, they found distinct task-relevant oscillatory activity in prefrontal and visual nodes, and that greater connectivity between ventral PFC and primary visual theta responses was associated with faster performance on the task (Wiesman *et al.*, 2017). In a later study, the same group showed that occipital-anodal tDCS significantly weakened the dynamic functional connectivity between right ventral PFC and visual cortex using the same visuospatial paradigm (Wiesman *et al.*, 2018). Building on this, we showed herein that anodal stimulation over left and right DLPFC differentially modulates fronto-visual networks in a lateralized manner, such that there is an increase in right DLPFC-visual networks when stimulating over the left DLPFC relative to the right DLPFC. These findings suggest that lateralized, focal stimulation may modulate theta oscillatory activity directly beneath the site of stimulation (i.e., DLPFC), its corresponding neural connections and most importantly, its homologous counterparts, especially when that site is of particular importance to task demands (i.e., right-hemispheric dominance during attention).

In conclusion, our findings indicate that right DLPFC-bilateral visual connections, but not left DLPFC-bilateral visual connections, are selectively modulated based on the laterality of DLPFC stimulation. Future studies should examine the specificity of these findings for visual-spatial processing and attention tasks, and determine if aging modulates this pattern. Given the known changes in the laterality of cognitive functions with age, one might predict that the laterality effects observed here would strongly decrease with advancing age and

thereby provide mechanistic evidence for the brain aging models that are now gaining wider acceptance (Cabeza, 2002; Cabeza *et al.*, 2002; Reuter-Lorenz PAC, 2008; Park & Reuter-Lorenz, 2009). To close, we selectively stimulated prefrontal cortices with HD-tDCS to infer mechanistic information on the distinct role of theta connectivity in left/right DLPFC-visual pathways in the context of visual selective attention. Our findings provide the first to clear evidence for a dynamic and systematic interplay between homologous DLPFC-visual networks in times of disruption (i.e., anodal tDCS) using state-of-the-art MEG recording and high definition neuromodulation.

Funding

This research was supported by grants RF1-MH117032 (TWW), R01-MH103220 (TWW), R01-MH116782 (TWW), and R01-MH118013 (TWW) from the National Institutes of Health, grant #1539067 from the National Science Foundation (TWW), the Shoemaker Prize from the University of Nebraska Foundation (TWW), and a grant from the Nebraska Banker's Association (TWW).

References

Bachtiar V, Near J, Johansen-Berg H & Stagg CJ. (2015). Modulation of GABA and resting state functional connectivity by transcranial direct current stimulation. Elife 4, e08789. [PubMed: 26381352]

Bikson M, Inoue M, Akiyama H, Deans JK, Fox JE, Miyakawa H & Jefferys JG. (2004). Effects of uniform extracellular DC electric fields on excitability in rat hippocampal slices in vitro. J Physiol 557, 175–190. [PubMed: 14978199]

Botvinick M, Nystrom LE, Fissell K, Carter CS & Cohen JD. (1999). Conflict monitoring versus selection-for-action in anterior cingulate cortex. Nature 402, 179–181. [PubMed: 10647008]

Brass M, Ullsperger M, Knoesche TR, von Cramon DY & Phillips NA. (2005). Who comes first? The role of the prefrontal and parietal cortex in cognitive control. J Cogn Neurosci 17, 1367–1375. [PubMed: 16197690]

Brookes MJ, Hale JR, Zumer JM, Stevenson CM, Francis ST, Barnes GR, Owen JP, Morris PG & Nagarajan SS. (2011). Measuring functional connectivity using MEG: methodology and comparison with fcMRI. Neuroimage 56, 1082–1104. [PubMed: 21352925]

Bunge SA, Hazeltine E, Scanlon MD, Rosen AC & Gabrieli JD. (2002). Dissociable contributions of prefrontal and parietal cortices to response selection. Neuroimage 17, 1562–1571. [PubMed: 12414294]

Busch NA, Dubois J & VanRullen R. (2009). The phase of ongoing EEG oscillations predicts visual perception. J Neurosci 29, 7869–7876. [PubMed: 19535598]

Cabeza R (2002). Hemispheric asymmetry reduction in older adults: the HAROLD model. Psychol Aging 17, 85–100. [PubMed: 11931290]

Cabeza R, Anderson ND, Locantore JK & McIntosh AR. (2002). Aging gracefully: compensatory brain activity in high-performing older adults. Neuroimage 17, 1394–1402. [PubMed: 12414279]

Carrasco M (2011). Visual attention: the past 25 years. Vision Res 51, 1484–1525. [PubMed: 21549742]

Cavanagh JF, Cohen MX & Allen JJ. (2009). Prelude to and resolution of an error: EEG phase synchrony reveals cognitive control dynamics during action monitoring. J Neurosci 29, 98–105. [PubMed: 19129388]

Cavanagh JF & Frank MJ. (2014). Frontal theta as a mechanism for cognitive control. Trends Cogn Sci 18, 414–421. [PubMed: 24835663]

Chao LL & Knight RT. (1995). Human prefrontal lesions increase distractibility to irrelevant sensory inputs. Neuroreport 6, 1605–1610. [PubMed: 8527724]

Chew T, Ho KA & Loo CK. (2015). Inter- and Intra-individual Variability in Response to Transcranial Direct Current Stimulation (tDCS) at Varying Current Intensities. Brain Stimul 8, 1130–1137. [PubMed: 26294061]

Coffman BA, Clark VP & Parasuraman R. (2014). Battery powered thought: enhancement of attention, learning, and memory in healthy adults using transcranial direct current stimulation. Neuroimage 85 Pt 3, 895–908. [PubMed: 23933040]

Cohen MX & Cavanagh JF. (2011). Single-trial regression elucidates the role of prefrontal theta oscillations in response conflict. Front Psychol 2, 30. [PubMed: 21713190]

Cohen MX & van Gaal S. (2014). Subthreshold muscle twitches dissociate oscillatory neural signatures of conflicts from errors. Neuroimage 86, 503–513. [PubMed: 24185026]

Corbetta M, Kincade JM, Ollinger JM, McAvoy MP & Shulman GL. (2000). Voluntary orienting is dissociated from target detection in human posterior parietal cortex. Nat Neurosci 3, 292–297. [PubMed: 10700263]

Corbetta M, Patel G & Shulman GL. (2008). The reorienting system of the human brain: from environment to theory of mind. Neuron 58, 306–324. [PubMed: 18466742]

Corbetta M & Shulman GL. (2002). Control of goal-directed and stimulus-driven attention in the brain. Nat Rev Neurosci 3, 201–215. [PubMed: 11994752]

Datta A, Baker JM, Bikson M & Fridriksson J. (2011). Individualized model predicts brain current flow during transcranial direct-current stimulation treatment in responsive stroke patient. Brain Stimul 4, 169–174. [PubMed: 21777878]

Datta A, Bansal V, Diaz J, Patel J, Reato D & Bikson M. (2009). Gyri-precise head model of transcranial direct current stimulation: improved spatial focality using a ring electrode versus conventional rectangular pad. Brain Stimul 2, 201–207, 207.e201. [PubMed: 20648973]

Datta A, Truong D, Minhas P, Parra L & Bikson M. (2012). Inter-individual variation during transcranial direct current stimulation and normalization of dose using MRI-derived computational models. Frontiers in Psychiatry 3, 8. [PubMed: 22347868]

Driver J (2001). A selective review of selective attention research from the past century. Br J Psychol 92 Part 1, 53–78.

Edwards D, Cortes M, Datta A, Minhas P, Wassermann EM & Bikson M. (2013). Physiological and modeling evidence for focal transcranial electrical brain stimulation in humans: a basis for high-definition tDCS. Neuroimage 74, 266–275. [PubMed: 23370061]

Embury CM, Wiesman AI, McDermott TJ, Proskovec AL, Heinrichs-Graham E, Lord GH, Brau KL, Drincic AT, Desouza CV & Wilson TW. (2018). The impact of type 1 diabetes on neural activity serving attention. Hum Brain Mapp.

Eriksen & Eriksen. (1974). Effects of noise letters upon identification of a target letter in a non-search task. Percept Psychophys 16, 7.

Ernst M (2004). Permutation Methods: A Basis for Exact Inference. Statistical Science 19, 10.

Fertonani A & Miniussi C. (2017). Transcranial Electrical Stimulation: What We Know and Do Not Know About Mechanisms. Neuroscientist 23, 109–123. [PubMed: 26873962]

Filmer HL, Dux PE & Mattingley JB. (2014). Applications of transcranial direct current stimulation for understanding brain function. Trends Neurosci 37, 742–753. [PubMed: 25189102]

Gregoriou GG, Rossi AF, Ungerleider LG & Desimone R. (2014). Lesions of prefrontal cortex reduce attentional modulation of neuronal responses and synchrony in V4. Nat Neurosci 17, 1003–1011. [PubMed: 24929661]

Gross J, Kujala J, Hamalainen M, Timmermann L, Schnitzler A & Salmelin R. (2001). Dynamic imaging of coherent sources: Studying neural interactions in the human brain. Proc Natl Acad Sci U S A 98, 694–699. [PubMed: 11209067]

Hanley CJ, Singh KD & McGonigle DJ. (2016). Transcranial modulation of brain oscillatory responses: A concurrent tDCS-MEG investigation. Neuroimage 140, 20–32. [PubMed: 26706447]

Hazeltine E, Poldrack R & Gabrieli JD. (2000). Neural activation during response competition. J Cogn Neurosci 12 Suppl 2, 118–129. [PubMed: 11506652]

Heilman KM & Van Den Abell T. (1980). Right hemisphere dominance for attention: the mechanism underlying hemispheric asymmetries of inattention (neglect). Neurology 30, 327–330. [PubMed: 7189037]

Heinrichs-Graham E, McDermott TJ, Mills MS, Coolidge NM & Wilson TW. (2017). Transcranial direct-current stimulation modulates offline visual oscillatory activity: A magnetoencephalography study. Cortex 88, 19–31. [PubMed: 28042984]

Huang Y, Dmochowski JP, Su Y, Datta A, Rorden C & Parra LC. (2013). Automated MRI segmentation for individualized modeling of current flow in the human head. J Neural Eng 10, 066004. [PubMed: 24099977]

Huang Y, Liu AA, Lafon B, Friedman D, Dayan M, Wang X, Bikson M, Doyle WK, Devinsky O & Parra LC. (2018). Correction: Measurements and models of electric fields in the. Elife 7.

Jasper HH. (1958). Electroencephalography and clinical neurophysiology, vol. 10.

Jensen O & Tesche CD. (2002). Frontal theta activity in humans increases with memory load in a working memory task. Eur J Neurosci 15, 1395–1399. [PubMed: 11994134]

Kaller CP, Rahm B, Spreer J, Weiller C & Unterrainer JM. (2011). Dissociable contributions of left and right dorsolateral prefrontal cortex in planning. Cereb Cortex 21, 307–317. [PubMed: 20522540]

Kempe R, Huang Y & Parra LC. (2014). Simulating pad-electrodes with high-definition arrays in transcranial electric stimulation. J Neural Eng 11, 026003. [PubMed: 24503644]

Kronberg G, Bridi M, Abel T, Bikson M & Parra LC. (2017). Direct Current Stimulation Modulates LTP and LTD: Activity Dependence and Dendritic Effects. Brain Stimul 10, 51–58. [PubMed: 28104085]

Kuo HI, Bikson M, Datta A, Minhas P, Paulus W, Kuo MF & Nitsche MA. (2013). Comparing cortical plasticity induced by conventional and high-definition 4 × 1 ring tDCS: a neurophysiological study. Brain Stimul 6, 644–648. [PubMed: 23149292]

Lachaux JP, Rodriguez E, Martinerie J & Varela FJ. (1999). Measuring phase synchrony in brain signals. Hum Brain Mapp 8, 194–208. [PubMed: 10619414]

Landau AN & Fries P. (2012). Attention samples stimuli rhythmically. Curr Biol 22, 1000–1004. [PubMed: 22633805]

Landau AN, Schreyer HM, van Pelt S & Fries P. (2015). Distributed Attention Is Implemented through Theta-Rhythmic Gamma Modulation. Curr Biol 25, 2332–2337. [PubMed: 26279231]

Lau H, Rogers RD & Passingham RE. (2006). Dissociating response selection and conflict in the medial frontal surface. Neuroimage 29, 446–451. [PubMed: 16150611]

Lennert T & Martinez-Trujillo J. (2011). Strength of response suppression to distracter stimuli determines attentional-filtering performance in primate prefrontal neurons. Neuron 70, 141–152. [PubMed: 21482363]

Lew BJ, McDermott TJ, Wiesman AI, O'Neill J, Mills MS, Robertson KR, Fox HS, Swindells S & Wilson TW. (2018). Neural dynamics of selective attention deficits in HIV-associated neurocognitive disorder. Neurology 91, e1860–e1869. [PubMed: 30333162]

Maris E & Oostenveld R. (2007). Nonparametric statistical testing of EEG- and MEG-data. J Neurosci Methods 164, 177–190. [PubMed: 17517438]

Marshall TR, Esterer S, Herring JD, Bergmann TO & Jensen O. (2016). On the relationship between cortical excitability and visual oscillatory responses - A concurrent tDCS-MEG study. Neuroimage 140, 41–49. [PubMed: 26455793]

McDermott TJ, Wiesman AI, Mills MS, Spooner RK, Coolidge NM, Proskovec AL, Heinrichs-Graham E & Wilson TW. (2019). tDCS modulates behavioral performance and the neural oscillatory dynamics serving visual selective attention. Hum Brain Mapp 40, 729–740. [PubMed: 30368974]

McDermott TJ, Wiesman AI, Proskovec AL, Heinrichs-Graham E & Wilson TW. (2017). Spatiotemporal oscillatory dynamics of visual selective attention during a flanker task. Neuroimage 156, 277–285. [PubMed: 28501539]

Miller BT & D'Esposito M. (2005). Searching for "the top" in top-down control. Neuron 48, 535–538. [PubMed: 16301170]

Miller EK. (2000). The prefrontal cortex and cognitive control. Nat Rev Neurosci 1, 59–65. [PubMed: 11252769]

Nigbur R, Cohen MX, Ridderinkhof KR & Stürmer B. (2012). Theta dynamics reveal domain-specific control over stimulus and response conflict. J Cogn Neurosci 24, 1264–1274. [PubMed: 21861681]

Nigbur R, Ivanova G & Stürmer B. (2011). Theta power as a marker for cognitive interference. Clin Neurophysiol 122, 2185–2194. [PubMed: 21550845]

Nitsche MA, Cohen LG, Wassermann EM, Priori A, Lang N, Antal A, Paulus W, Hummel F, Boggio PS, Fregni F & Pascual-Leone A. (2008). Transcranial direct current stimulation: State of the art 2008. Brain Stimul 1, 206–223. [PubMed: 20633386]

Nitsche MA, Nitsche MS, Klein CC, Tergau F, Rothwell JC & Paulus W. (2003). Level of action of cathodal DC polarisation induced inhibition of the human motor cortex. Clin Neurophysiol 114, 600–604. [PubMed: 12686268]

Nitsche MA & Paulus W. (2000). Excitability changes induced in the human motor cortex by weak transcranial direct current stimulation. J Physiol 527 Pt 3, 633–639. [PubMed: 10990547]

Nitsche MA & Paulus W. (2001). Sustained excitability elevations induced by transcranial DC motor cortex stimulation in humans. Neurology 57, 1899–1901. [PubMed: 11723286]

Okamoto M, Dan H, Sakamoto K, Takeo K, Shimizu K, Kohno S, Oda I, Isobe S, Suzuki T, Kohyama K & Dan I. (2004). Three-dimensional probabilistic anatomical cranio-cerebral correlation via the international 10–20 system oriented for transcranial functional brain mapping. Neuroimage 21, 99–111. [PubMed: 14741647]

Okamoto M & Dan I. (2005). Automated cortical projection of head-surface locations for transcranial functional brain mapping. Neuroimage 26, 18–28. [PubMed: 15862201]

Padrão G, Rodriguez-Herreros B, Pérez Zapata L & Rodriguez-Fornells A. (2015). Exogenous capture of medial-frontal oscillatory mechanisms by unattended conflicting information. Neuropsychologia 75, 458–468. [PubMed: 26151855]

Paneri S & Gregoriou GG. (2017). Top-Down Control of Visual Attention by the Prefrontal Cortex. Functional Specialization and Long-Range Interactions. Front Neurosci 11, 545. [PubMed: 29033784]

Park DC & Reuter-Lorenz P. (2009). The adaptive brain: aging and neurocognitive scaffolding. Annu Rev Psychol 60, 173–196. [PubMed: 19035823]

Posner MI & Petersen SE. (1990). The attention system of the human brain. Annu Rev Neurosci 13, 25–42. [PubMed: 2183676]

Radman T, Su Y, An JH, Parra LC & Bikson M. (2007). Spike timing amplifies the effect of electric fields on neurons: implications for endogenous field effects. J Neurosci 27, 3030–3036. [PubMed: 17360926]

Reato D, Rahman A, Bikson M & Parra LC. (2010). Low-intensity electrical stimulation affects network dynamics by modulating population rate and spike timing. J Neurosci 30, 15067–15079. [PubMed: 21068312]

Reuter-Lorenz PAC K (2008). Neurocognitive aging and the compensation hypothesis. Current Directions in Psychological Science 17, 6.

Ruffini G, Fox MD, Ripolles O, Miranda PC & Pascual-Leone A. (2014). Optimization of multifocal transcranial current stimulation for weighted cortical pattern targeting from realistic modeling of electric fields. Neuroimage 89, 216–225. [PubMed: 24345389]

Shulman GL, Pope DL, Astafiev SV, McAvoy MP, Snyder AZ & Corbetta M. (2010). Right hemisphere dominance during spatial selective attention and target detection occurs outside the dorsal frontoparietal network. J Neurosci 30, 3640–3651. [PubMed: 20219998]

Spooner RK, Wiesman AI, Mills MS, O'Neill J, Robertson KR, Fox HS, Swindells S & Wilson TW. (2018a). Aberrant oscillatory dynamics during somatosensory processing in HIV-infected adults. Neuroimage Clin 20, 85–91. [PubMed: 30094159]

Spooner RK, Wiesman AI, Proskovec AL, Heinrichs-Graham E & Wilson TW. (2018b). Rhythmic Spontaneous Activity Mediates the Age-Related Decline in Somatosensory Function. Cereb Cortex 29, 680–688.

Spooner RK, Wiesman AI, Proskovec AL, Heinrichs-Graham E & Wilson TW. (2019). Prefrontal theta modulates sensorimotor gamma networks during the reorienting of attention. Hum Brain Mapp [Epub ahead of print].

Suzuki M & Gottlieb J. (2013). Distinct neural mechanisms of distractor suppression in the frontal and parietal lobe. Nat Neurosci 16, 98–104. [PubMed: 23242309]

Taulu S & Simola J. (2006). Spatiotemporal signal space separation method for rejecting nearby interference in MEG measurements. Phys Med Biol 51, 1759–1768. [PubMed: 16552102]

Taulu S, Simola J & Kajola M. (2005). Applications of the Signal Space Separation Method. IEEE Transactions on Signal Processing 53, 3359–3372.

Turski CA, Kessler-Jones A, Chow C, Hermann B, Hsu D, Jones J, Seeger SK, Chappell R, Boly M & Ikonomidou C. (2017). Extended Multiple-Field High-Definition transcranial direct current stimulation (HD-tDCS) is well tolerated and safe in healthy adults. Restor Neurol Neurosci 35, 631–642. [PubMed: 29172010]

Uusitalo MA & Ilmoniemi RJ. (1997). Signal-space projection method for separating MEG or EEG into components. Med Biol Eng Comput 35, 135–140. [PubMed: 9136207]

Van Veen B, van Drongelen W, Yuchtman M & Suzuki A. (1997). Localization of brain electrical activity via linearly constrained minimum variance spatial filtering. IEEE Trans Biomed Eng 44, 867–880. [PubMed: 9282479]

van Veen V, Cohen JD, Botvinick MM, Stenger VA & Carter CS. (2001). Anterior cingulate cortex, conflict monitoring, and levels of processing. Neuroimage 14, 1302–1308. [PubMed: 11707086]

Verbruggen F, Aron AR, Stevens MA & Chambers CD. (2010). Theta burst stimulation dissociates attention and action updating in human inferior frontal cortex. Proc Natl Acad Sci U S A 107, 13966–13971. [PubMed: 20631303]

Wiesman AI, Heinrichs-Graham E, Proskovec AL, McDermott TJ & Wilson TW. (2017). Oscillations during observations: Dynamic oscillatory networks serving visuospatial attention. Hum Brain Mapp 38, 5128–5140. [PubMed: 28714584]

Wiesman AI, Mills MS, McDermott TJ, Spooner RK, Coolidge NM & Wilson TW. (2018). Polarity-dependent modulation of multi-spectral neuronal activity by transcranial direct current stimulation. Cortex 108, 222–233. [PubMed: 30261367]

Wilson TW, Kurz MJ & Arpin DJ. (2014). Functional specialization within the supplementary motor area: a fNIRS study of bimanual coordination. Neuroimage 85 Pt 1, 445–450. [PubMed: 23664948]

Wilson TW, McDermott TJ, Mills MS, Coolidge NM & Heinrichs-Graham E. (2018). tDCS Modulates Visual Gamma Oscillations and Basal Alpha Activity in Occipital Cortices: Evidence from MEG. Cereb Cortex 28, 1597–1609. [PubMed: 28334214]

Key points summary

- Visual attention involves discrete multispectral oscillatory responses in visual and “higher-order” prefrontal cortices.
- Prefrontal cortex laterality effects during visual selective attention are poorly characterized.
- HD-tDCS dynamically modulated right-lateralized fronto-visual theta oscillations compared to those observed in left fronto-visual pathways.
- Increased connectivity in right fronto-visual networks after stimulation of the left DLPFC resulted in faster task performance in the context of distractors.
- Our findings show clear laterality effects in theta oscillatory activity along prefrontal-visual cortical pathways during visual selective attention.

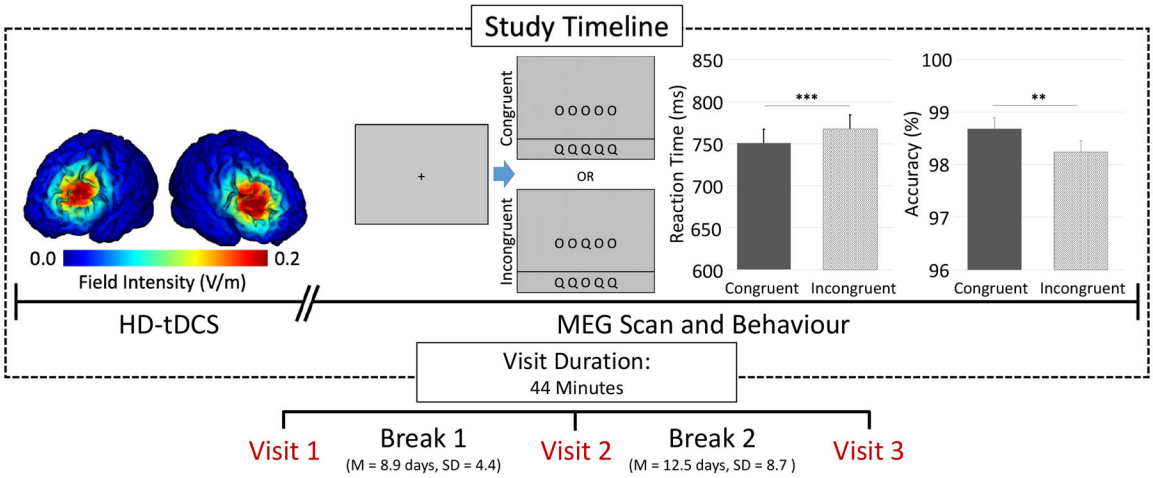

Figure 1. Study design, current density modeling, and behavioral results.

Participants completed 20 minutes of anodal and sham HD-tDCS over the left and right DLPFC, followed by completion of a modified Eriksen Flanker task during MEG. Each visit lasted for ~44 minutes (from HD-tDCS setup to completion of MEG recording) and was separated by at least 7 days, with stimulation montages pseudo-randomized across all visits. Current density modeling of prefrontal montages revealed a relatively focal distribution of field intensity over the left and right DLPFC (left). Performance on the modified Eriksen flanker task (middle) showed a significant interference effect across all HD-tDCS stimulation montages, such that participants were less accurate and slower during incongruent relative to congruent trials ($p < .01$; right).

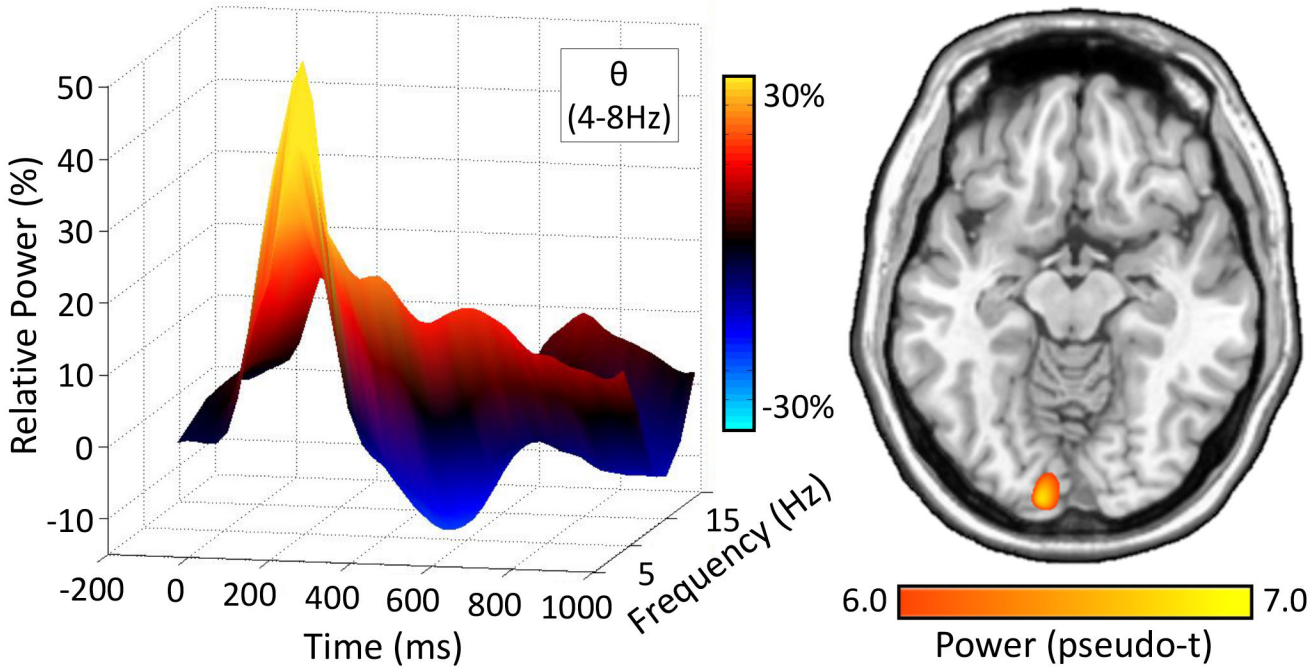

Figure 2. Theta Activity during Visual Selective Attention.

(Left): 3D Time-frequency spectrogram from a MEG sensor near the occipital cortices, with stimulus onset occurring at 0 ms. Time (ms) is depicted on the x-axis, with relative power (%) on the y-axis, and frequency (Hz) on the z-axis. All signal power data is expressed as percent change from baseline (−450 to −50 ms), and the corresponding color scale bar is displayed to the right of the graphic. (Right): Grand averaged beamformer images (pseudo-t) across all participants, HD-tDCS montages and task conditions. Strong increases in theta power were found in virtually identical primary visual regions across both conditions and the different stimulation montages.

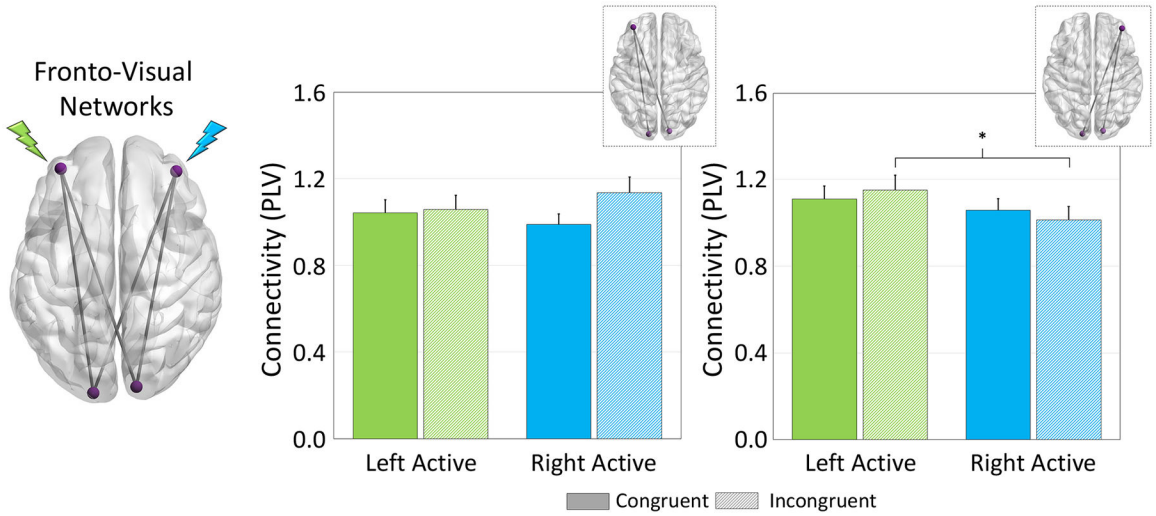

Figure 3. HD-tDCS Modulation of Fronto-Visual Networks.

(Left): The glass brain represents all functional networks interrogated (e.g., left DLPFC-left and right visual). Phase coherence among sites of stimulation during target processing were evaluated by extracting the phase-locking value (PLV; normalized to sham) and averaged over the task active period for each pathway, and then averaged across left/right occipital pathways for the left DLPFC and Right DLPFC separately. (Right) Sites of stimulation are noted in green and blue for the left- and right-DLPFC, respectively. A significant montage × condition × network interaction was apparent in the right DLPFC-bilateral visual network (far right) such that dynamic functional connectivity between right DLPFC and bilateral visual cortices was increased during processing of incongruent trials when participants underwent left DLPFC stimulation (shown in green) compared to right ($p = .043$). Further, there were no significant effects of tDCS configuration or task condition on left DLPFC-bilateral visual network connectivity (left graphs: p's > .20). *$p < .05$